

Bubbleless Air Shapes Biofilms and Facilitates Natural Organic Matter Transformation in Biological Activated Carbon

Mengjie Liu, Nigel J. D. Graham, Lei Xu, Kai Zhang, and Wenzheng Yu*



Cite This: <https://doi.org/10.1021/acs.est.2c08889>



Read Online

ACCESS |

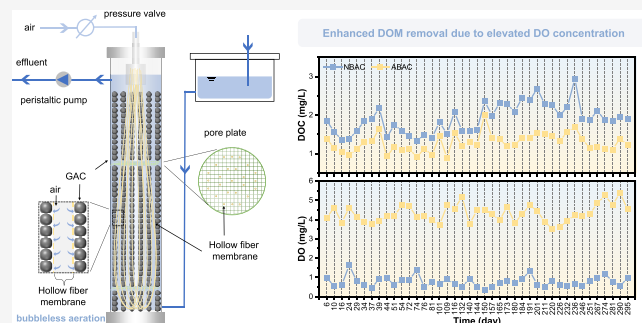
Metrics & More

Article Recommendations

Supporting Information

ABSTRACT: The biodegradation in the middle and downstream of slow-rate biological activated carbon (BAC) is limited by insufficient dissolved oxygen (DO) concentrations. In this study, a bubbleless aerated BAC (termed ABAC) process was developed by installing a hollow fiber membrane (HFM) module within a BAC filter to continuously provide aeration throughout the BAC system. The BAC filter without an HFM was termed NBAC. The laboratory-scale ABAC and NBAC systems operated continuously for 426 days using secondary sewage effluent as an influent. The DO concentrations for NBAC and ABAC were 0.78 ± 0.27 and 4.31 ± 0.44 mg/L, respectively, with the latter providing the ABAC with greater electron acceptors for biodegradation and a microbial community with better biodegradation and metabolism capacity. The biofilms in ABAC secreted 47.3% less EPS and exhibited greater electron transfer capacity than those in NBAC, resulting in enhanced contaminant degradation efficiency and long-term stability. The extra organic matter removed by ABAC included refractory substances with a low elemental ratio of oxygen to carbon (O/C) and a high elemental ratio of hydrogen to carbon (H/C). The proposed ABAC filter provides a valuable, practical example of how to modify the BAC technology to shape the microbial community, and its activity, by optimizing the ambient atmosphere.

KEYWORDS: *biological activated carbon (BAC), bubbleless aeration, natural organic matter (NOM), hollow fiber aeration*



1. INTRODUCTION

In the context of increasing water pollution, diminishing water resources, and the rising demand for high-quality drinking water, municipal wastewater effluents are being recognized as a potential future source of drinking water.¹ However, the indirect, or direct, recycling of municipal wastewater may expose humans and the environment to harmful organic pollutants. Therefore, advanced treatment processes should be performed to remove dissolved organic matter (DOM) and hazardous/detrimental substances from secondary wastewater effluents, either prior to environmental discharge or upstream of reclamation processes.

Biofiltration is an effective water treatment technology, based partially or entirely upon biological degradation. It can be broadly divided into natural and engineered processes.² Natural biofiltration (e.g., riverbank and aquifer filtration) is widely used for water environment remediation, with a hydraulic retention time (HRT) of several days to a few months.³ Engineered biofiltration, using filter media (e.g., sand, granular activated carbon (GAC)) as carriers of biofilms, is more prevalent in water treatment plants due to its higher rate of treatment (measured as substrate reduction per unit area, unit time) and thus low physical footprint. Biofiltration using GAC as a filter material, also known as the biological activated carbon (BAC) process, has been recognized as a versatile

technology for achieving a high degree of removal of a variety of contaminants, such as biodegradable and recalcitrant DOM, ammonia, emerging micropollutants, and taste and odor compounds, from water.^{4–7} In drinking water treatment, BAC is a potential alternative technology to conventional coagulation as a chemical-free pretreatment for ultrafiltration (UF), especially for small-scale drinking water systems.⁸ The process removes particulate matter and biopolymers (the most important organic pollutants causing membrane fouling), ensuring drinking water safety and improving the sustainability of UF.⁹ Pre-ozone can facilitate the DOM removal rate of BAC by improving the biodegradability of DOM and elevating the dissolved oxygen concentration (DO) in BAC influents. This combination (O_3 –BAC) has been successfully applied to advanced drinking water treatment¹⁰ and decentralized wastewater reuse.^{11–13}

Despite the success of BAC in a variety of water treatment applications, the HRT of BAC in most water treatment plants

Received: November 28, 2022

Revised: February 19, 2023

Accepted: February 21, 2023

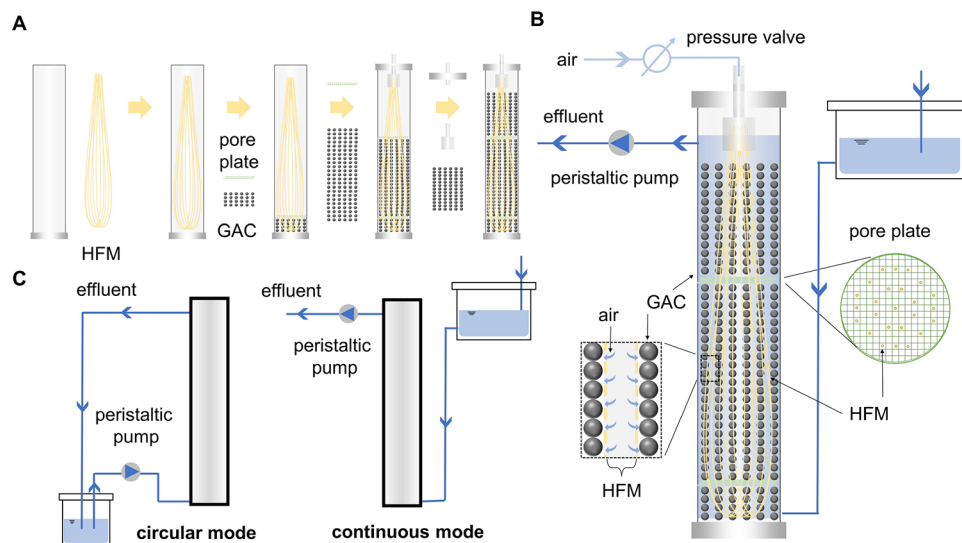


Figure 1. (A) Schematic showing assembly of the ABAC system. (B) Operation diagram of the ABAC system. (C) Two operation modes (circular and continuous) of the BAC systems.

is typically short (less than 30 min) to reduce the physical footprint. As a result, the NOM removal rate is relatively low (i.e., 12% (median) removal of the influent DOC with a 12 min (average) HRT¹⁴), and regular backwashing is required to cope with clogging and head loss accumulation.¹⁵ Our previous study used GAC with larger particle sizes (3 to 5 mm diameter) to construct a biofilter and found that when the HRT was prolonged to 24 h, the DOM removal could reach approximately 80%.¹⁶ The large GAC size avoided severe clogging that can occur in conventional high-rate biofilters (with a GAC diameter of 1 to 2 mm). Therefore, no backwash was needed during over 400 day operation.¹⁶ This kind of operation mode, termed as gravity-driven up-flow slow biofilter, has the advantages of low energy consumption, low maintenance, and high efficiency and is a sustainable choice for small-scale, decentralized wastewater purification and reclamation.

Nonetheless, one of the most challenging problems for BAC lies in the progressive consumption of DO through the filter depth, which results in anoxic conditions and poor degradation efficiency in the middle and downstream regions of the process.^{17,18} It has been reported that up-flow BAC filters showed enhanced biological activities due to a greater oxygen availability than their downflow counterparts.^{7,19} Some studies have considered aeration of the influent with pure oxygen to enhance the biological degradation in BAC,^{4,9} but the aeration is energy-consuming. Therefore, a method that can provide uniform oxygen throughout the BAC system is necessary for the sustainable application of the BAC process. In recent years, “bubbleless aeration”, where pressurized gas diffuses into the solution through the membrane module without forming bubbles, has been applied to activated sludge systems and hydrolysis acidification processes.^{20,21} Compared to bubble aeration, it has the advantage of uniform mass transfer, low supply pressure, and a low operation cost.^{20,22,23} Herein, we applied this concept to the BAC process and proposed a bubbleless aerated BAC filter for the advanced treatment of secondary wastewater effluents. The hollow fiber membrane module (HFM) strips were placed evenly in the activated carbon column to ensure uniform distribution of air throughout the filter. The objectives of this study are as

follows: (1) to investigate DOM transformation during the BAC process; (2) to examine the enhancement of DOM removal by BAC via bubbleless aeration; and (3) to explore the effects of DO on the biofilm structure as well as the DOM degradation mechanism. The results from this study have emphasized the importance of oxygen in slow-rate biofiltration and provided an approach for supplementing DO and enhancing the performance of a fixed-bed biotreatment system.

2. MATERIALS AND METHODS

2.1. Experimental Setup and Operation Modes. Two parallel circular plexiglass columns (diameter: 50 mm × height: 500 mm) were packed with granular activated carbon (GAC, average particle size of 3–5 mm) to serve as the lab-scale BAC systems. The packed bed height was 450 mm, and the GAC particle volume was 300 mL, corresponding to a bed porosity of 0.66. A polyvinylidene difluoride (PVDF) hollow fiber membrane (HFM, diameter: 1.1 mm) module with 18 strips of HFM was installed with a U-shape in one of the columns to continuously provide air, without bubbling, to the BAC system, which was termed ABAC (bubbleless aerated BAC filter), and the other column, without HFM modules, was termed NBAC (non-aerated BAC filter). To maintain a uniform air distribution, each strip of HFM was separated from others by several pore plates incorporated in the column, as shown in Figure 1A,B.

The BAC system could operate in both circular (re-cycle) and continuous (single pass) modes by changing the arrangement of pipe fittings, connections, and storage tank (Figure 1C). When working in circular mode, the feed water was pumped to the column using a peristaltic pump with two channels (L100-1S-1-DG-6, Longer pump, China); the water flowed upward from the column bottom and then gravitated back from the top of the column to the feed water tank. For the continuous flow, a tank with a constant water level was used to maintain the water level of the filter column; the feed water flowed upward from the bottom through the column, and a peristaltic pump was used to draw the water at a constant rate.

2.2. Raw Water and Continuous Operation. The raw water in this study was sourced from a local lake (Olympic

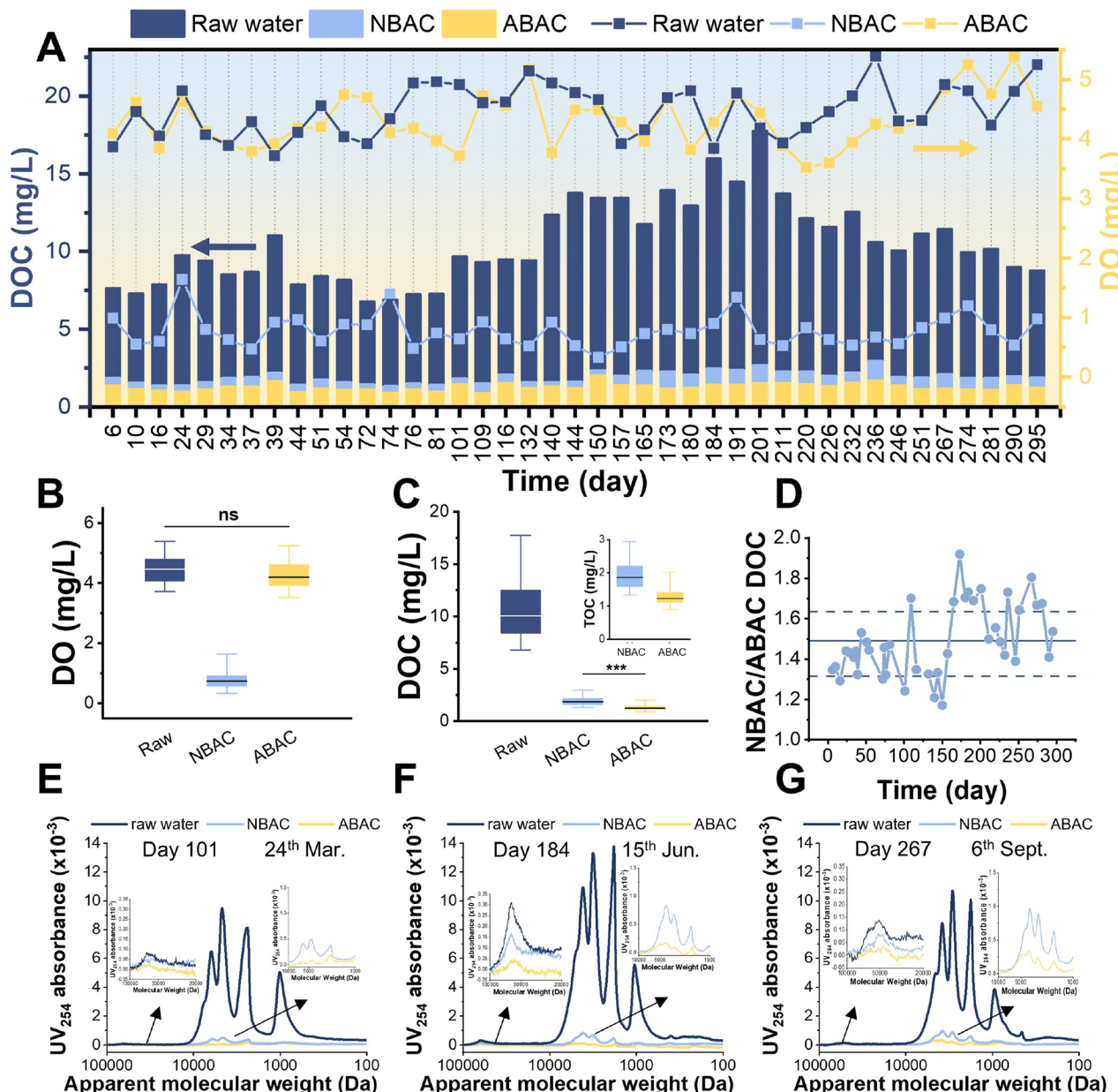


Figure 2. Water quality of raw water and the effluents from the two BAC systems in the first phase (HRT = 12 h). (A) Variation in DOC and DO values with operation time. Box plot showing the (B) DOC and (C) DO of raw water (Raw), NBAC effluent, and ABAC effluent (The box plot displays the six-number summary of a set of data: centerline, median; box limits, upper and lower quartiles; whiskers, 1.5× interquartile range; points, outliers. A paired Student's *t* test was conducted between two groups: ***, *p* < 0.001, ns, *p* > 0.05.). (D) DOC value ratio (NBAC/ABAC), where the solid line indicates the average value, and the dashed lines represent the averaged value ± standard deviation. Apparent molecular weight distribution for raw water and effluents at (E) day 101, (F) day 184, and (G) day 267.

Park, Beijing, China), which comes from the secondary effluent of a sewage plant and is used as landscape water for the Olympic Park. Detailed information on the OP water is listed in the Supporting Information (SI, Table S1). Prior to treating OP water, the BAC filters were inoculated with micro-organisms using soil from the OP lakeside and then operated for two weeks to pre-stabilize the performance of the BAC filters. Details about microbial inoculation and pre-operation of the BAC filters are also described in the SI (Text S1). Subsequently, the OP water was used as feed water, and the two BAC systems were operated continuously for four different phases: (1) HRT of 12 h for 300 days (bed approach velocity, v_a = 1.27 cm/h); (2) HRT of 6 h (v_a = 2.55 cm/h) for six

weeks; (3) HRT of 4 h for six weeks (v_a = 3.82 cm/h); (4) HRT of 12 h (v_a = 1.27 cm/h) for six weeks. All experiments were conducted at room temperature (20–24 °C). The performance of two BAC filters on DOM removal was comprehensively compared during the first period (Sections 3.1–3.3). The effect of HRT on DOM removal efficiency was explored in Section 3.4.

3.3. Water Quality Measurements. Water samples were collected from the constant level water tank (R, raw water) and from the outlet of the ABAC (A) and NBAC (N) filters and were then filtered by a membrane filter (SCAA-201, 25 mm × 0.22 μm, ANPEL) prior to the following measurements. Dissolved organic carbon (DOC) and UV-visible absorbance

spectra were measured by a total organic carbon analyzer (TOC-Vwp, Shimadzu, Japan) and UV spectrometer (UV-2600, Shimadzu, Japan), respectively. A high-performance liquid chromatography (HPLC) system (Waters, USA) was used to analyze the molecular weight (MW) distribution. Dissolved oxygen (DO) was determined using a FiveGo DO meter (Mettler Toledo, USA). Water samples from the middle of the BAC systems (200 mm below the water surface) were collected for DO measurement. 3D excitation–emission matrix (EEM) spectrofluorometry (F-4600FL, HITACHI, Japan) was used to characterize the fluorescent components. For this, the elimination of scattering, the correction of the inner filter effect and intensity, and parallel factor (PARAFAC) analysis were applied to the EEM data using the R software package Stadom.²⁴ The EEM spectra were divided into five wavelength regions, and their integrals were calculated according to a previous study.²⁵ Several optical parameters were calculated from the EEM and UV–visible spectral data, as shown in the SI (Table S2). A principal component analysis (PCA) was conducted using the R community ecology package, “vegan”.²⁶ The measurements of DOC, UV, and DO were replicated three times at each test, and all the water quality tests (including EEM and MW distribution tests) were conducted once a week on average.

Disinfection byproduct (DBP) formation potential (DBPFP) was based on the widely regulated trihalomethane and haloacetic acid compounds. These were determined by a gas chromatograph (Clarus 590, PerkinElmer, U.S.) with an electron capture detector (ECD), following the U.S. Environmental Protection Agency methods 551 and 552.3.^{27,28} Details of the methods are included in the SI (Texts S2 and S3). The measurements of DBPFP were replicated three times for each sample. Solid phase extraction (SPE) was performed using Agilent Bond Elute PPL cartridges, and the recovery rates were 59.7 to 64.3%. Subsequently, Fourier transform ion resonance cyclotron mass spectrometry (FT-ICR-MS) analysis was conducted using a Bruker SolariX FT-ICR-MS instrument equipped with a 15.0 T superconducting magnet and an ESI ion source. The procedures for SPE and FT-ICR-MS are available in the SI (Text S4).

2.4. Chemical Characterization of Biofilms on Activated Carbon. At the end of the test period, the GAC particles from the middle of the two columns (150–300 mm below the water level) were removed and rinsed twice with 0.01 M phosphoric acid buffer (PBS, containing 3.2 mM Na₂HPO₄, 0.5 mM KH₂PO₄, 1.3 mM KCl, and 135 mM NaCl, pH = 7.4) for subsequent chemical and microbial characterization. The electrochemical properties of the GAC particles were measured using an electrochemical station (Gamry, Interface 1010E, USA) (SI, Text S5). The electrochemical impedance spectrum (EIS) results were fitted using Zview software (ZiffNet, USA). Scanning electron microscopy (SEM, JSM-7001F + INCA X-MAX, Japan) was employed for morphological characterization (SI, Text S6). Extracellular polymeric substances (EPS) were extracted from GAC particles using the heating method as described in our previous study (SI, Text S7),¹ and the polysaccharide and protein contents within the EPS were quantified via spectrophotometry methods.^{29,30} The measurements were replicated three times.

2.5. Microbial Community Analysis. At the end of test period, GAC particles from the top (100 mm below the water surface), middle (200 mm below the water surface), and

bottom (300 mm below the water surface) sections were taken out (2 g from each section) and mixed. After the pretreatments (SI, Text S8), the samples were divided into three replicates for subsequent DNA extraction and 16S rRNA sequencing. Procedures for DNA extraction and 16S rRNA sequencing are described in the SI (Text S8). A neutral community model (NCM) was used to describe how much of the variation in the microbial communities could be determined by a neutral stochastic process.³¹ Linear discriminant analysis Effect Size (LEfSe) was performed on the Galaxy platform, and the linear discriminant analysis (LDA) threshold was set at 4.³² A phylogenetic investigation of communities, by reconstruction of unobserved states (PICRUSt2),³³ was conducted using the online tool of the Majorbio Cloud Platform.³⁴ The relationship between samples and microbial species was demonstrated by Circos.³⁵ Other data processing and plotting exercises were conducted in Origin 2021 and R 4.1.0.³⁶ The significance was evaluated by a Wilcoxon test: ns, $p \geq 0.05$; *, $0.01 \leq p < 0.05$; **, $0.001 \leq p < 0.01$; ***, $p < 0.001$.

3. RESULTS

3.1. Long-Term Effluent Quality. After pre-stabilization, the two filters (ABAC and NBAC) operated continuously at an HRT of 12 h for 300 days (from 13th December 2020 to 9th October 2021). The ABAC system showed DO values comparable to those of the raw water (ABAC: 4.31 ± 0.44 mg/L; raw water: 4.47 ± 0.43 mg/L), while the DO of the NBAC system decreased to 0.78 ± 0.27 mg/L due to the gradual consumption of DO by microbial activities (Figure 2B and SI, Figure S2). DO has been reported to be an essential factor affecting the biological degradation of organic matter, which serves as an electron acceptor in biological redox reactions and can thereby support the growth of heterotrophic bacteria along with the degradation of organic carbon.³⁷ As a result, the DOC of effluents from the ABAC and NBAC filters showed substantial differences, with the latter (1.90 ± 0.38 mg/L) being approximately 1.5 times that of the former (1.28 ± 0.23 mg/L) (Figure 2C,D).

The seasonal variation in raw water would be expected to affect the performance of BAC systems.¹² Here, the BAC systems operated at room temperature, and therefore, the composition of the raw water was the main factor responsible for the process performance. As shown in Figure 2A, the DOC of the raw water showed a significant increase after day 140, which might be attributed to flushing of the organic soil horizons in the wet season.³⁸ Figure 2E–G and Figure S3 in the SI show the molecular weight (MW) distribution of the raw water and BAC effluents at different operation times. At day 101 (24th March 2021), the biopolymer content (10–100 kDa) in the raw water was very low, and the differences in biopolymer content between the raw water and the two effluents were minor (Figure 2E). However, at day 184 (15th June 2021), a substantial increase in biopolymers in the raw water was observed due to the intense microbial activity in the wet season, and ABAC exhibited a much greater removal of biopolymers than NBAC (Figure 2F). In addition, the amount of mid-MW substances (1–10 kDa) in the NBAC effluent increased substantially from day 101 to day 184, with the peak value (MW at around 5000 Da) increased by 1.65 times. There are two possible reasons for this result: first, the organic burden in the raw water increased and exceeded the removal capability of the NBAC; second, the removal efficiency of NBAC decreased with time. Moreover, from day 184 to day 267, the

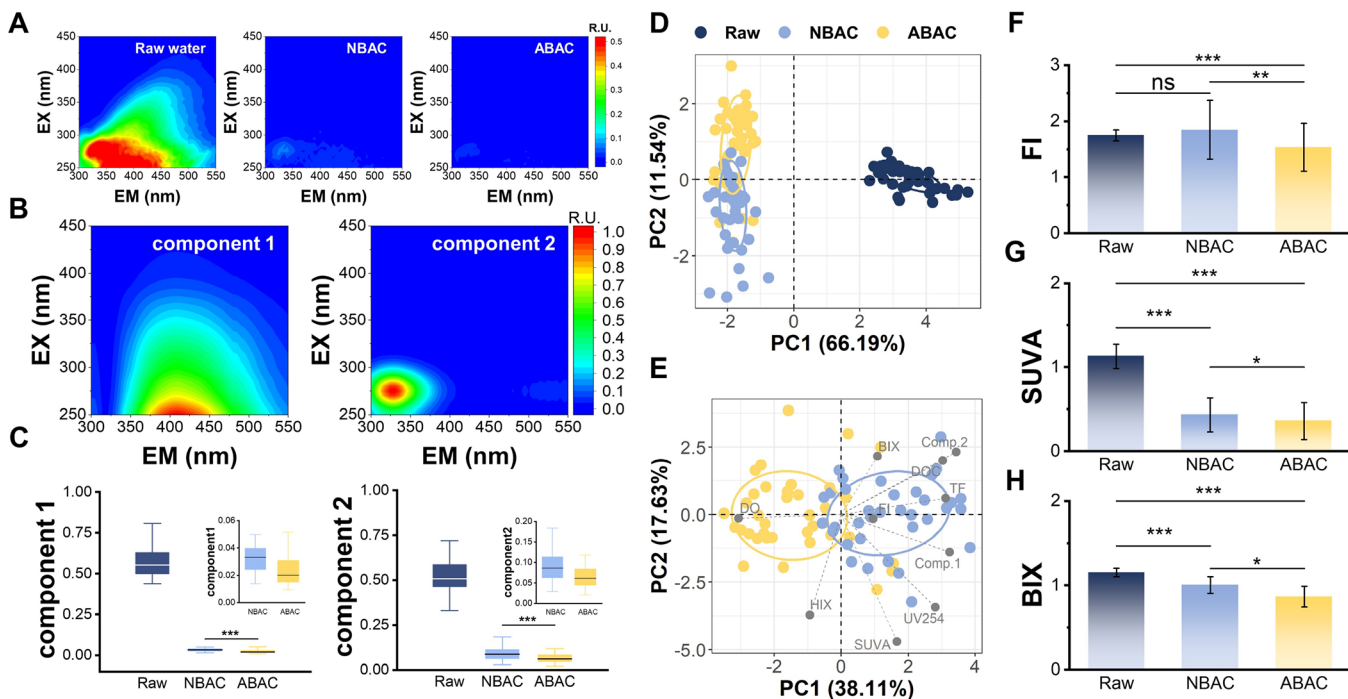


Figure 3. Absorbance properties of DOM in raw water and effluents from the two BAC systems. (A) EEM spectra of raw water (left), NBAC effluent (middle), and ABAC effluent (right). (B) Loadings of two fluorescence components identified using PARAFAC. (C) EEM intensity of component 1 (left) and component 2 (right) in raw water (Raw), NBAC effluent, and ABAC effluent (The box plot displays the six-number summary of a set of data: centerline, median; box limits, upper and lower quartiles; whiskers, 1.5× interquartile range; points, outliers. A Wilcoxon test was conducted between two groups: ***, $p < 0.001$.). PCA results showing the difference (D) among raw water (dark blue), NBAC effluent (light blue), and ABAC effluent (yellow) and (E) between the two BAC effluents (The gray points in E are water indexes: DOC, DO, ultraviolet absorbance at 254 nm (UV₂₅₄), dissolved organic carbon specific ultraviolet absorbance at 254 nm (SUVA), fluorescence index (FI), biological index (BIX), humification index (HIX), TF (total fluorescence), and two PARAFAC components (Comp. 1 and Comp. 2).). (F) FI, (G) SUVA, and (H) BIX of raw water (Raw), NBAC effluent, and ABAC effluent (The error bars indicate the standard deviation. The Wilcoxon test was conducted between each pair of groups: ***, $p < 0.001$; **, $0.001 < p < 0.01$; *, $0.01 < p < 0.05$; ns, $p > 0.05$).

organic matter content in the raw water decreased, but the amount of mid-MW substances in the NBAC effluent still increased, while, in contrast, there was only a small increase for the ABAC system. These results confirmed that the removal efficiency of NBAC gradually decreased with operation time. In addition, the variation of UV₂₅₄ also confirmed that the difference between the NBAC effluent and ABAC effluent, respectively, gradually increased with time (SI, Figure S4). Therefore, it can be concluded that ABAC had a greater performance and stability during long-term operation.

3.2. Absorbance Properties of DOM. The absorbance properties of DOM changed substantially after BAC treatments. The total fluorescence (TF) decreased to 12.0 and 7.3% after NBAC and ABAC of raw water, respectively (Figure 3A). Parallel factor (PARAFAC) analysis identified two independent fluorescence components: one humic-like³⁹ (C1) and one protein-like⁴⁰ (C2) (Figure 3B and SI, Figure S5). ABAC showed a significant increase in the removal of both components compared to NBAC (Figure 3C). A previous study using slow-rate biofiltration to treat secondary wastewater effluent suggested that biopolymers were more preferably removed than humic substances.¹⁸ However, our results demonstrated a high removal rate of humic substances. This result might be ascribed to the high concentration of humic acid (HA) solution used as feed water at the initial adsorption stage (SI, Text S1), which favored the enrichment of HA-degrading microorganisms. Principal component analysis (PCA) suggested that raw water samples separated

from BAC effluents at the first principal axis, which accounted for 66.19% of the total variance. NBAC and ABAC samples were separated along the second principal axis, with 11.54% explained variance (Figure 3D). We took a closer look at the water samples from the two systems via another round of PCA, with only NBAC and ABAC samples considered. As shown in Figure 3E, NBAC samples and ABAC samples were distributed on the positive and negative sides of the first principal axis, respectively. Water indexes that represent the content of DOM (i.e., DOC, TF) clustered at the positive side of the first principal axis, indicating that ABAC had a better removal of DOM than NBAC. The fluorescence index (FI) is an index used to identify the relative contributions of terrestrial and microbial sources to the DOM pool.⁴¹ The significant differences in FI between ABAC and raw water, and, more importantly, between ABAC and NBAC implied a more intense microbial activity in the ABAC system than in NBAC due to the uniform and high DO concentration (Figure 3F). The specific UV absorbance (SUVA) and biological index (BIX) were distributed along the second principal axis, and the Wilcoxon test showed that there were differences between the two systems for these two indexes ($p < 0.05$). SUVA describes the aromatic content in water, and the biodegradation of humic acid resulted in a decrease in SUVA (Figure 3G). BIX is an indicator of autotrophic productivity; high values of BIX (>1) correspond to freshly released DOM from autochthonous origin into water, whereas a low BIX (0.6–0.7) indicates low DOM production (Figure 3H).⁴² Therefore, a higher removal

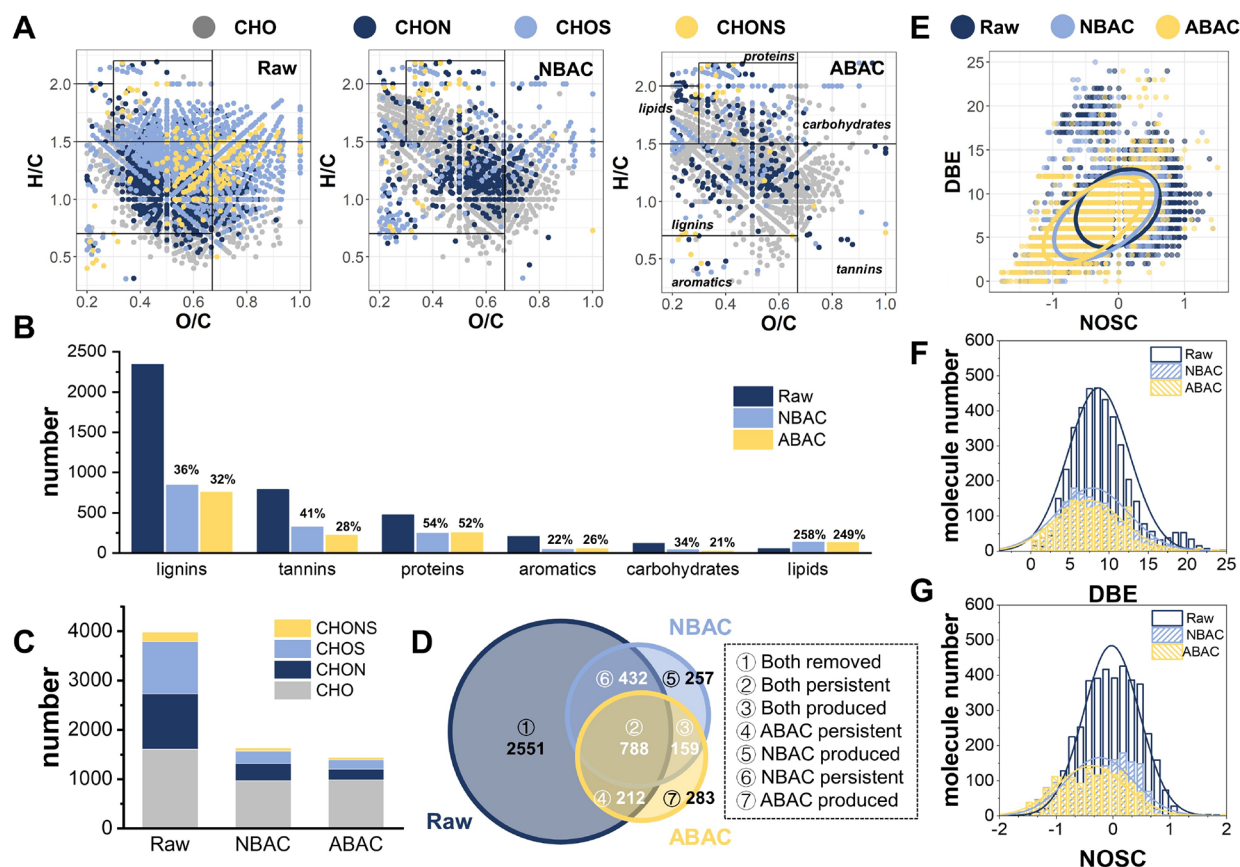


Figure 4. (A) Van Krevelen (VK) diagrams of DOM in raw water (left), NBAC effluent (middle), and ABAC effluent (right) (Boxes overlain on the plots indicate major compound classes: lipids, proteins, carbohydrates, lignins, aromatics, and tannins.). (B) Molecule numbers of compound classes in raw water (Raw, dark blue), NBAC effluent (light blue), and ABAC effluent (yellow) (The numbers indicate the ratio of molecule number treated by BAC to raw water.). (C) Molecule numbers of element composition: CHO (gray), CHON (dark blue), CHOS (light blue), and CHONS (yellow). (D) Venn diagram showing the molecule number in seven groups: both removed, both persistent, both produced, NBAC removed, NBAC produced, ABAC removed, ABAC produced. (E) NOSC and DBE of molecules in raw water (Raw, dark blue), NBAC effluent (light blue), and ABAC effluent (yellow). Distribution of (F) DBE and (G) NOSC.

of freshly produced OM components was observed in ABAC compared to NBAC.

3.3. Molecular Transformation. Fourier transform ion resonance cyclotron mass spectrometry (FT-ICR-MS) is a powerful technique to examine the molecular composition of DOM and has been widely employed to analyze the molecular transformation during different water treatments.⁴³ After careful formula assignment, 3983, 1636, and 1442 peaks were determined for raw water, NBAC effluent, and ABAC effluent, respectively. The Van Krevelen (VK) diagrams (Figure 4A) can be divided into several compound classes.^{44–47} Lignins were the major compound type in raw water, and the molecule numbers decreased to 36 and 32% after NBAC and ABAC treatments, respectively (Figure 4B). Significant reductions in molecule numbers were also observed for tannins, proteins, aromatics, and carbohydrates. However, the number of molecules with low O/C and high H/C (lipids) increased, suggesting poor biological degradation of pre-existing lipids or/and the production of lipids via microbial activities.⁴⁸ From the perspective of element composition, molecules that only contained C, H, and O elements accounted for 40% of the total molecule numbers in raw water, which increased to 59 and 68% after NBAC and ABAC treatment, respectively (Figure 4C). This suggested that the BAC systems could effectively treat organics with N- and S-

containing functional groups, and ABAC outperformed NBAC in treating these substances due to its higher DO.⁴⁹

The Venn diagram, displayed in Figure 4D, illustrates the number of molecules removed and produced by the two BAC systems. Among the 3893 molecules in raw water, 2551 molecules were removed by both BAC systems, and 788 molecules were persistent in both BAC systems. ABAC and NBAC produced 442 and 416 new molecules, respectively, and 159 of them were identical. Additionally, NBAC alone removed 212 molecules and produced 257 molecules, while ABAC alone removed 432 molecules and produced 283 molecules. Detailed discussion about the molecular properties of these seven groups are available in the SI (Text S9) and Figure S6. The normal oxidation state of carbon (NOSC)⁵⁰ and double bond equivalence (DBE) were used to further characterize the redox potential and the number of double bonds in molecules, respectively. After BAC treatments, both NOSC and DBE shifted to lower values (Figure 4E). A previous study suggested that the intrinsic molecular properties were important for the overall organic matter reactivity.⁵¹ Specifically, DOM with a highly oxidized state and aromatic structures were preferentially removed by biogeochemical degradation processes.⁵¹ Therefore, reduced (low NOSC) and aliphatic (low DBE) compounds were the major components in BAC effluents. Compared to NBAC, the shift of NOSC and

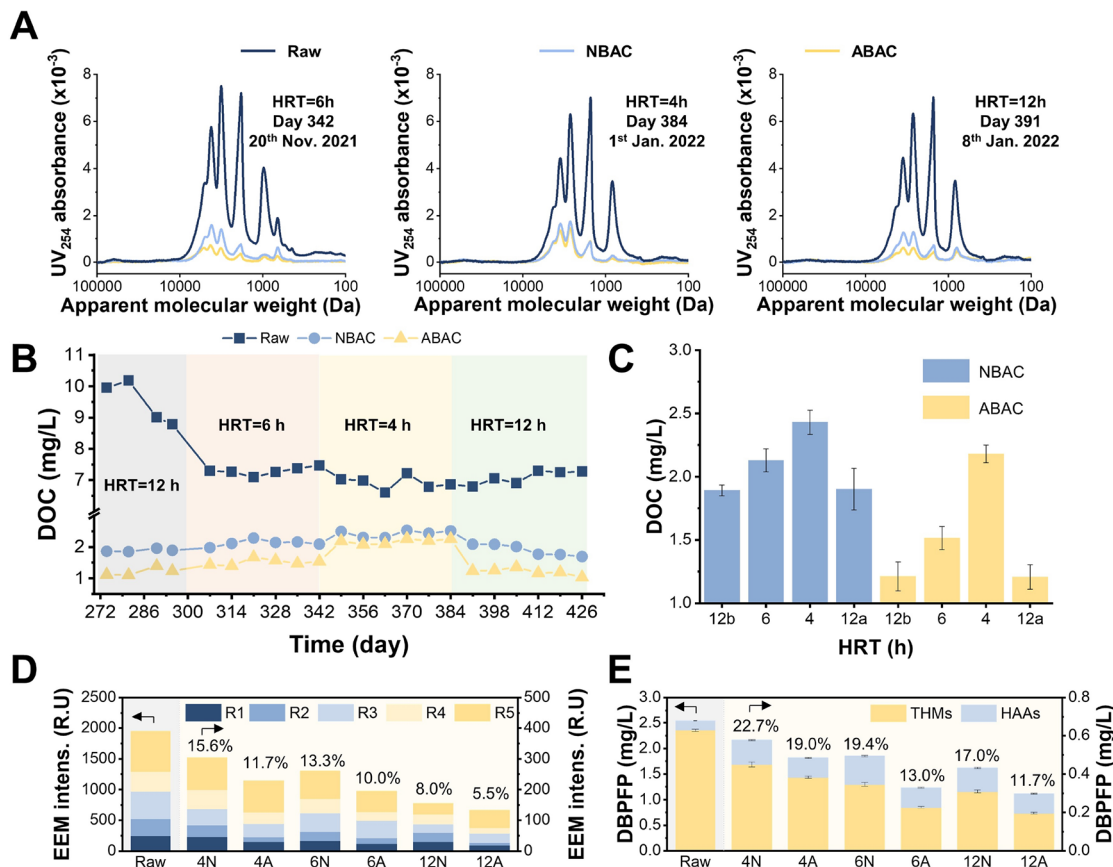


Figure 5. Performance of BAC systems with different hydraulic retention times (HRTs). (A) Apparent molecular weight distribution for raw water and effluents at HRTs of 6 h (left), 4 h (middle), and 12 h (right). (B) Variation in DOC values with operation time (The HRT was 6 h from day 301 to 342, 4 h from day 343 to 384, and 12 h from day 385 to 426.). (C) Variation of DOC for NBAC (blue) and ABAC (yellow) effluents with HRTs of 12, 6, and 4 h (The error bar represents one standard deviation.). The label “12a” indicated the 12 h period after HRT changing, while “12b” indicated the 12 h period before the 6 h period. (D) Intensity (intens.) of five EEM components for raw water and BAC effluents (The % numbers indicate the ratio of EEM intensity of water treated by BAC to raw water. The five EEM components are R1: tyrosine-like aromatic protein, R2: tryptophan-like aromatic protein, R3: fulvic acid-like matter, R4: soluble microbial byproduct-like matter, and R5: humic acid-like matter (SI, Table S4)). (E) DBP formation potential (DBPFP) for raw water and BAC effluents, based on four trihalomethanes (THMs) and eight haloacetic acids (HAAs) (SI, Table S4 and Figure S8) (The % numbers indicate the ratio of DBPFP of water treated with BAC to raw water.). The x axis labels in Figure 5D,E indicate the HRT (4, 6, and 12 h) and BAC treatments (N for NBAC and A for ABAC). In panel D and E, the left y axis represents the values for the Raw, and the right y axis represents the values for the 4N, 4A, 6N, 6A, 12N, and 12A bars in the revised paper.

DBE to lower values in the ABAC system was more pronounced (Figure 4F,G), indicating the enhanced removal efficiency of refractory compounds due to the bubbleless aeration.

3.4. Effect of Hydraulic Retention Time. Hydraulic retention time (HRT) is a key factor that determines BAC performance by affecting the nutrient load of microorganisms. After operating at an HRT of 12 h for 300 days, the HRT was changed to 6 h for six weeks and then decreased to 4 h for another six weeks. To exclude the influences of raw water quality differences and the reduction in treatment performance of the BAC filters over time, the HRT was subsequently returned to 12 h, and the results of this period as well as ~ 30 days before the 6 h period were used for the comparison of BAC performances under different HRTs. As shown in Figure 5A, although there was a slight reduction in UV_{254} in the raw water as the HRT decreased from 6 to 4 h, both the NBAC and ABAC effluents showed a rise in UV_{254} , and the difference between the two systems decreased. This indicated that the DO concentration in the influent was sufficient for the whole BAC system as the HRT was shortened to 4 h. However, when the HRT returned to 12 h, the DOM removal rate increased,

and the differences between the two filters increased again. The variation of DOC under different HRTs is summarized in Figure 5B,C. The effluent DOC increased as the HRT shortened for both BAC systems, indicating that the contact time limited the degradation of recalcitrant DOM. However, the DOC for the ABAC filter under an HRT of 6 h was still lower than the DOC for the NBAC filter under an HRT of 12 h, indicating that the ABAC system could treat twice as much water as NBAC while maintaining the quality of the effluent. In other words, the physical footprint can be halved when using the ABAC process. Both BAC systems achieved a substantial reduction of EEM intensity, with 84.4 to 94.5% removal rates under different HRTs (Figure 5D and SI, Figure S7). Regarding the removal of DBP precursors, 12 DBPs (four THMs and eight HAAs) were detected in this study (SI, Figure S8). Among these 12 DBPs, a striking decrease with increasing HRT was noticed for TCM, DCBM, CDBA, and TBAA, while little variation or some increase occurred for the remaining eight DBPs. Overall, the DBP formation potential (DBPFP) increased as the HRT was shortened, but the ABAC under an HRT of 6 h still outperformed the NBAC under an HRT of 12 h (Figure 5E).

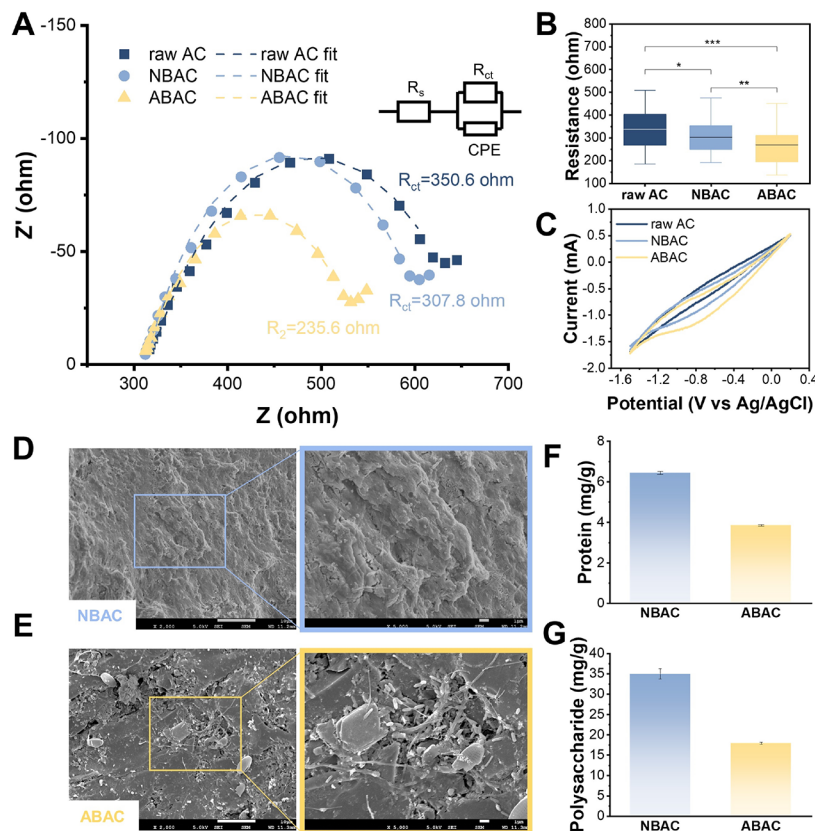


Figure 6. Characterization of GAC particles. (A) Nyquist plots of EIS for raw GAC and BAC particles from NBAC and ABAC filters. (The inset shows the equivalent circuit of the arc section. The dashed line represents the fitting line. R_{ct} is the charge transfer resistance value, and the fitting results are labeled.). (B) R_{ct} values for raw GAC, NBAC, and ABAC particles, each with 20 replicates (The box plot displays the six-number summary of a set of data: centerline, median; box limits, upper and lower quartiles; whiskers, 1.5× interquartile range; points, outliers. The Wilcoxon test was conducted between each pair of groups, and the significance is labeled: *, 0.01 < p < 0.05, **, 0.001 < p < 0.1, ***, p < 0.001.). (C) Cyclic voltammograms of GAC, NBAC, and ABAC particles. Surface morphology of (D) NBAC and (E) ABAC particles. (F) Protein and (G) polysaccharide content of EPS from NBAC and ABAC particles. Error bars represent the standard deviation.

3.5. Characterization of GAC. At the end of the period of operation, the GAC particles within the two systems were taken out and characterized. The Nyquist plots of EIS are shown in Figure 6A. The curve can be divided into two parts: the semicircular arc in the high frequency region and the straight line in the low frequency region, which represent the charge transfer reaction and the diffusion of ions at the interface between the electrode and solution, respectively. A smaller semicircle in the high frequency region reflected a smaller charge transfer resistance in the interface region.⁵² As shown in the inset of Figure 6A, an equivalent circuit model, composed of electrolyte resistance (R_s), a constant phase element (CPE), and charge transfer resistance (R_{ct}), was used to fit the semicircular arc part of the EIS with Zview software.⁵³ Based on the fitting results, the charge transfer resistance for ABAC (235.6 ohm) was lower than those for raw GAC (350.6 ohm) and NABC (307.8 ohm), suggesting faster charge transfer across the interface between the solution and the ABAC particles. Due to the variety in size and shape, the charge transfer resistance of GAC particles (from the same system) showed some differences. Therefore, twenty GAC particles were taken from each system to measure the charge transfer resistance, and the results are shown in Figure 6B. The Wilcoxon test indicated that the median charge transfer resistance of the ABAC system was significantly lower than those of the raw GAC and NBAC systems. Figure 6C shows

the cyclic voltammograms of GAC particles. There were no apparent redox peaks, and the area of the CV curve was strongly correlated with the double layer capacitance. The results showed that ABAC had a larger double layer capacitance than NBAC, implying that it could provide more electrochemically active sites for the adsorption of pollutants. As a consequence, ABAC outperformed NBAC in terms of both degradation rate and degradation capacity, thus providing more favorable conditions for the degradation of DOM by microbial activities.

The SEM results revealed apparent morphological differences between the carbon particles from the NBAC and ABAC filters. As shown in Figure 6D,E and Figure S9 (SI), the surface of BAC particles from NBAC was completely covered by dense biofilms, where the bacteria were wrapped by the EPS. In contrast, individual bacteria can be easily distinguished on the surface of ABAC particles due to less secreted EPS, principally polysaccharides and proteins (Figure 6F,G). It can be observed that there were filamentous junctions between cells on both ABAC and NBAC particles. Previous studies have suggested that some bacteria secrete proteinaceous pilin filaments with widths of 3–5 nm, which can grow tens of micrometers long and serve as nanowires to transport electrons over long distances.^{54–56} This might explain the lower charge transfer resistance observed for ABAC (Figure 6A,B). However, for NBAC, the filamentous structures were covered by the EPS,

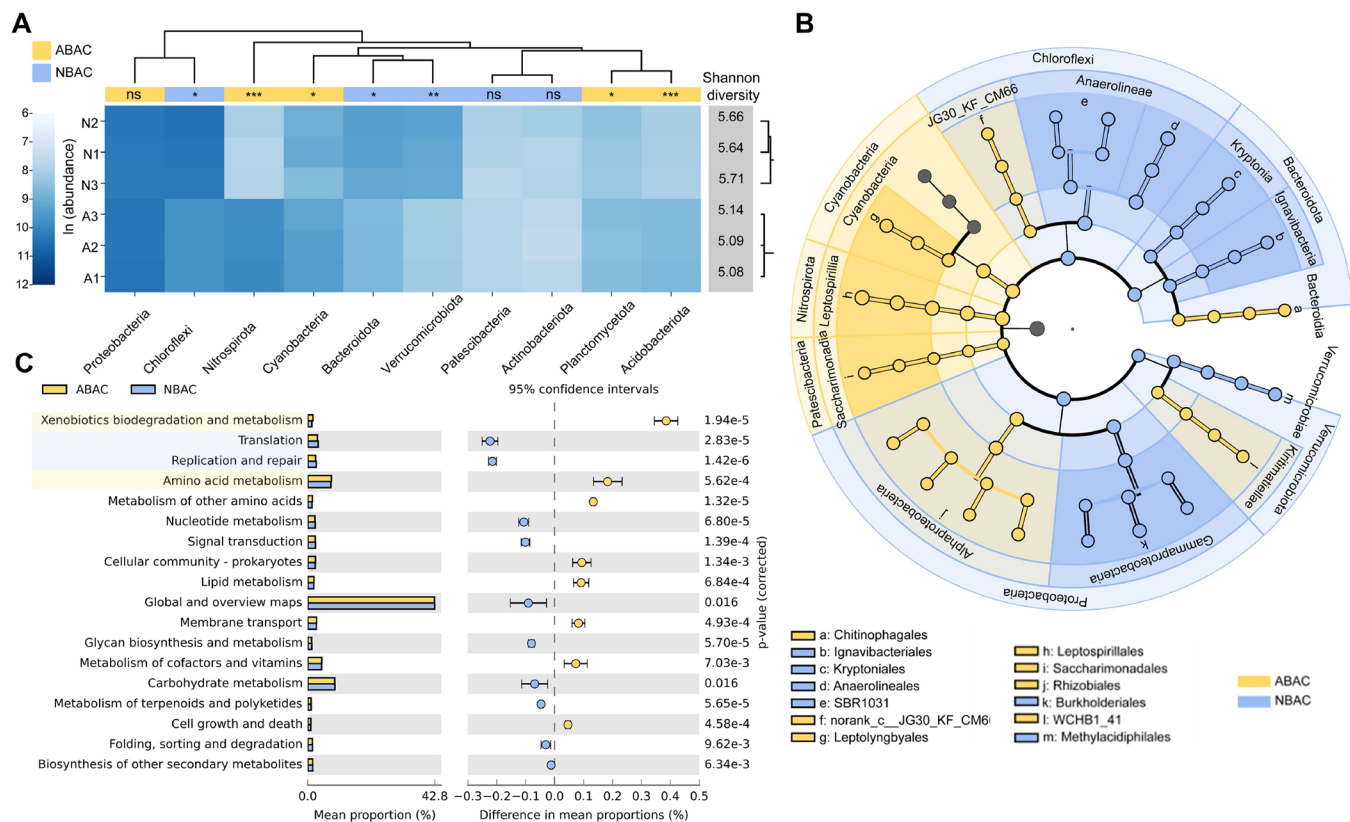


Figure 7. Microbial community of the two BAC systems. (A) Heatmap illustrating the relative abundances of bacterial communities at the phylum level (top 10) based on 16S rRNA sequencing (N1–N3 are the three NBAC samples, and A1–A3 are the three ABAC samples. Shannon diversity is labeled on the right side of each sample. The bar colors (blue and yellow) indicate the groups with higher abundance (NBAC or ABAC), and the significance was evaluated by a Wilcoxon test: ns, $p \geq 0.05$; *, $0.01 \leq p < 0.05$; **, $0.001 \leq p < 0.01$; ***, $p < 0.001$). (B) Cladogram showing the phylogenetic distribution of the bacterial lineages (Indicator bacteria with LDA scores of four or greater in bacterial communities were highlighted in yellow and blue, indicating that they are significantly abundant in the ABAC and NBAC groups, respectively.). (C) Extended bar plot showing the function prediction results by PICRUSt2 at KEGG level 2 (ABAC and NABC groups were compared by Welch's *t*-test, and the *p*-value was labeled at the right side. Categories with a *p*-value greater than 0.05 were not shown).

which has been reported to hinder extracellular electron transfer.⁵⁷

3.6. Microbial Community. Microorganisms play an essential role in the long-term stable operation of BAC. The differences in the microbial community compositions of the two BAC systems are likely to be responsible for the disparity in DOM removal efficiency. The neutral theory recognizes that the microbial community structure is determined by random processes such as birth, death, migration, and diffusion.⁵⁸ In contrast, many studies try to explain the differences in microbial community structure in terms of environmental factors, caused mainly by deterministic processes. The neutral community model qualifies the importance of neutral processes (stochastic processes) in the community assembly. According to the results in Figure S10 in the SI, the NCM explained 76.0 and 68.5% of the community variation in the NBAC and ABAC filters, respectively, suggesting that neutral processes were dominant in the microbial community assembly. However, a lower prediction accuracy for ABAC also implied that DO served as a deterministic selection to affect the microbial community assembly in the BAC filter. In addition, ABAC showed a lower alpha diversity than NBAC (Figure 7A and SI, Table S5), implying that the more uniform DO throughout the filter bed prevented the stratification of the microbial community, which occurred in the conventional BAC system. PCoA ordinations showed great differences in the

bacterial community compositions between the ABAC and NBAC filters (SI, Figure S11). Differences in the proportions among species composition were quite significant (evaluated by Wilcoxon test, $p < 0.05$) at the phylum level (Figure 7A). *Proteobacteria*, with 24 and 29% relative abundance in the NBAC and ABAC filters, respectively, was the most abundant phylum identified in both BAC systems. However, LEfSe results ($\text{LDA} > 4$) indicated that the two systems differed at *Proteobacteria* subcategories (Figure 7B and SI, Figure S12): *Alphaproteobacteria* was significantly enriched in ABAC, which have been reported to be competitive under low nutrient concentrations and can degrade complex organic compounds, such as humic acid.^{59,60} On the contrary, NBAC had more *Gammaproteobacteria*, and a previous study has suggested that members of *Gammaproteobacteria* showed a fast growth rate, especially in the presence of nitrogen and phosphorus.⁶¹ Additionally, the ABAC community was significantly enriched with *Nitrospirota* ($p < 0.001$), an aerobic bacterium that can decrease the concentration of ammonia nitrogen and nitrite, indicating that the enhanced DO in the ABAC filter can also favor the nitrification process in the BAC filters.⁶²

Based on the functional annotation from PICRUSt analysis (Figure 7C), the KEGG pathways differed between the two BAC systems. Notably, global and overview maps—accounting for 42.8% mean proportion of all pathways—were the most abundant pathway at KEGG level 2 followed by carbohydrate

metabolism, amino acid metabolism, and energy metabolism, which, respectively, accounted for 9.1, 7.9, 5.3, and 4.7% of all pathways. Comparing the two systems, the results revealed that NBAC outperformed on translation, replication, and repair, while ABAC showed significantly higher abundance on xenobiotics biodegradation and metabolism and amino acid metabolism, which was consistent with the FT-ICR-MS results wherein ABAC favored the removal of N-containing organic matter (Figure 7C). Moreover, among the sub-functional categories of global and overview maps, ABAC exhibited higher abundance at microbial metabolism in a diverse environment, and NBAC was better at biosynthesis processes (SI, Figure S13). All these results demonstrated that ABAC had the advantage of microbial degradation, while the activities associated with biosynthesis and microbial growth were more prevalent in NBAC. The results of functional prediction were in good agreement with the characterizations in the above sections and explained the greater removal efficiency in the ABAC system.

4. IMPLICATIONS

In this study, an enhanced BAC process (termed ABAC) was developed by installing a hollow fiber membrane module within a conventional BAC filter bed (termed NBAC) to continuously and uniformly provide bubbleless aeration for biological degradation. The elevated dissolved oxygen concentration in ABAC enabled the microbial community to exhibit a greater biodegradation capacity, facilitated a biofilm with less secreted EPS and an improved electron transfer capability. As a consequence, the ABAC filter outperformed the conventional NBAC filter for the removal of DOM and stability for long-term operation.

Biological processes are environmentally sustainable and hold the prospect of being predominant in water treatment. However, the mineralization of DOM by microorganisms usually takes a relatively long time, which leads to a trade-off between removal efficiency, and the physical footprint, of the process. By regulating the ambient conditions, the microbial communities and their activities can be promoted to enhance biodegradation efficiency. Here, we promote the degradation of DOM by providing oxygen (electron acceptor) to the system, reaching a higher DOC removal efficiency than non-aerated BAC even if the HRT is shortened by half. The advantages of this device are being low maintenance and highly efficient. Although the footprint limitation should be further discussed for the application of slow-rate BAC in modern water treatment plants, this system has the potential to be applied to decentralized water treatment and in situ water environment restoration, where the processes can be implemented in rural areas with sufficient space resources or embedded urban ecological water bodies such as wetland parks. For instance, it could replace riverbank filtration or trickling filters that are used in many rural Chinese villages. In addition, the proposed technology can also be designed for anoxic or anaerobic biodegradation processes by providing different atmospheres (e.g., nitrogen). Moreover, this study provides a potential solution to the degradation of specific pollutants by regulating the process atmosphere to promote the growth of dominant microorganisms.

ASSOCIATED CONTENT

SI Supporting Information

The Supporting Information is available free of charge at <https://pubs.acs.org/doi/10.1021/acs.est.2c08889>.

(Text 1) microbial inoculation and pre-operation of the BAC filters; (Text S2) chemical standards for DBP calibration; (Text S3) measurement of DBPFP; (Text S4) FT-ICR-MS analysis details; (Text S5) electrochemical properties of GAC particles; (Text S6) pretreatments before SEM characterization; (Text S7) extraction of EPS from GAC particles; (Text S8) details for 16s RNA analysis; (Figure S1) absorbance at 254 nm during pre-stabilization section; (Figure S2) DO–filter height profiles for the NBAC and ABAC systems; (Figure S3) enlarged plots of high-MW and mid-MW fraction; (Figure S4) variation of UV₂₅₄ (cm⁻¹) with operation time; (Figure S5) variation of EEM components; (Figure S6) difference in molecular transformation between the two systems; (Figure S7) EEM spectra of raw water and BAC effluents under different HRTs; (Figure S8) DBP formation potential (DBPFP) for raw water (Raw) and BAC effluents; (Figure S9) morphological characterization of biofilms on NBAC and ABAC particles; (Figure S10) NCM analyses; (Figure S11) overall principal coordinate analysis (PCoA) of bacterial communities; (Figure S12) relative abundance of the bacteria across different samples at the class level; (Figure S13) extended bar plot showing the function prediction results by PICRUSt2 at KEGG level 3; (Table S1) physical and chemical properties of OP water; (Table S2) abbreviations for water quality indexes; (Table S3) detailed information of DBPs; (Table S4) molecular parameters; (Table S5) alpha diversity ([PDF](#))

AUTHOR INFORMATION

Corresponding Author

Wenzheng Yu – State Key Laboratory of Environmental Aquatic Chemistry, Key Laboratory of Drinking Water Science and Technology, Research Center for Eco-Environmental Sciences, Chinese Academy of Sciences, Beijing 100085, People's Republic of China;  orcid.org/0000-0001-9776-8021; Email: wzyu@rcees.ac.cn

Authors

Mengjie Liu – State Key Laboratory of Environmental Aquatic Chemistry, Key Laboratory of Drinking Water Science and Technology, Research Center for Eco-Environmental Sciences, Chinese Academy of Sciences, Beijing 100085, People's Republic of China; University of Chinese Academy of Sciences, Beijing 100049, People's Republic of China

Nigel J. D. Graham – Department of Civil and Environmental Engineering, Imperial College London, London SW7 2AZ, U.K.

Lei Xu – State Key Laboratory of Environmental Aquatic Chemistry, Key Laboratory of Drinking Water Science and Technology, Research Center for Eco-Environmental Sciences, Chinese Academy of Sciences, Beijing 100085, People's Republic of China;  orcid.org/0000-0003-2240-0737

Kai Zhang – State Key Laboratory of Environmental Aquatic Chemistry, Key Laboratory of Drinking Water Science and

Technology, Research Center for Eco-Environmental Sciences, Chinese Academy of Sciences, Beijing 100085, People's Republic of China

Complete contact information is available at:
<https://pubs.acs.org/10.1021/acs.est.2c08889>

Notes

The authors declare no competing financial interest.

ACKNOWLEDGMENTS

This work was financially supported by the Beijing Natural Science Foundation (No. 8192042), a Marie Curie International Incoming Fellowship (FP7-PEOPLE-2012-IIF-328867) within the 7th European Community Framework Programme, and the Key Research and Development Plan of the Chinese Ministry of Science and Technology (No. 2019YFD1100104 and No. 2019YFC1906501).

REFERENCES

- (1) Xiong, X.; Bond, T.; Saboor Siddique, M.; Yu, W. The stimulation of microbial activity by microplastic contributes to membrane fouling in ultrafiltration. *J. Membr. Sci.* **2021**, *635*, 119477.
- (2) Kirisits, M. J.; Emelko, M. B.; Pinto, A. J. Applying biotechnology for drinking water biofiltration: advancing science and practice. *Curr. Opin. Biotechnol.* **2019**, *57*, 197–204.
- (3) Zucker, I.; Mamane, H.; Cikurel, H.; Jekel, M.; Hübner, U.; Avisar, D. A hybrid process of biofiltration of secondary effluent followed by ozonation and short soil aquifer treatment for water reuse. *Water Res.* **2015**, *84*, 315–322.
- (4) Reungoat, J.; Escher, B. I.; Macova, M.; Keller, J. Biofiltration of wastewater treatment plant effluent: Effective removal of pharmaceuticals and personal care products and reduction of toxicity. *Water Res.* **2011**, *45*, 2751–2762.
- (5) Rattier, M.; Reungoat, J.; Gernjak, W.; Joss, A.; Keller, J. Investigating the role of adsorption and biodegradation in the removal of organic micropollutants during biological activated carbon filtration of treated wastewater. *Journal of Water Reuse and Desalination* **2012**, *2*, 127–139.
- (6) Wang, C.; Gallagher, D. L.; Dietrich, A. M.; Su, M.; Wang, Q.; Guo, Q.; Zhang, J.; An, W.; Yu, J.; Yang, M. Data Analytics Determines Co-occurrence of Odorants in Raw Water and Evaluates Drinking Water Treatment Removal Strategies. *Environ. Sci. Technol.* **2021**, *55*, 16770–16782.
- (7) Rui, M.; Chen, H.; Ye, Y.; Deng, H.; Wang, H. Effect of Flow Configuration on Nitrifiers in Biological Activated Carbon Filters for Potable Water Production. *Environ. Sci. Technol.* **2020**, *54*, 14646–14655.
- (8) Hallé, C.; Huck, P. M.; Peldszus, S.; Haberkamp, J.; Jekel, M. Assessing the Performance of Biological Filtration As Pretreatment to Low Pressure Membranes for Drinking Water. *Environ. Sci. Technol.* **2009**, *43*, 3878–3884.
- (9) Chang, H.; Yu, H.; Li, X.; Zhou, Z.; Liang, H.; Song, W.; Ji, H.; Liang, Y.; Vidic, R. D. Role of biological granular activated carbon in contaminant removal and ultrafiltration membrane performance in a full-scale system. *J. Membr. Sci.* **2022**, *644*, 120122.
- (10) Phungsai, P.; Kurisu, F.; Kasuga, I.; Furumai, H. Changes in Dissolved Organic Matter Composition and Disinfection Byproduct Precursors in Advanced Drinking Water Treatment Processes. *Environ. Sci. Technol.* **2018**, *52*, 3392–3401.
- (11) Shi, J. L.; Plata, S. L.; Kleimans, M.; Childress, A. E.; McCurry, D. L. Formation and Fate of Nitromethane in Ozone-Based Water Reuse Processes. *Environ. Sci. Technol.* **2021**, *55*, 6281–6289.
- (12) Hess, A.; Morgenroth, E. Biological activated carbon filter for greywater post-treatment: Long-term TOC removal with adsorption and biodegradation. *Water Research X* **2021**, *13*, 100113.
- (13) Jantararakasem, C.; Kasuga, I.; Kurisu, F.; Furumai, H. Temperature-Dependent Ammonium Removal Capacity of Biological Activated Carbon Used in a Full-Scale Drinking Water Treatment Plant. *Environ. Sci. Technol.* **2020**, *54*, 13257–13263.
- (14) Terry, L. G.; Summers, R. S. Biodegradable organic matter and rapid-rate biofilter performance: A review. *Water Res.* **2018**, *128*, 234–245.
- (15) Piche, A.; Campbell, A.; Cleary, S.; Douglas, I.; Basu, O. D. Investigation of backwash strategy on headloss development and particle release in drinking water biofiltration. *Journal of Water Process Engineering* **2019**, *32*, 100895.
- (16) Xu, L.; Zhou, Z.; Graham, N. J. D.; Liu, M.; Yu, W. Enhancing ultrafiltration performance by gravity-driven up-flow slow biofilter pre-treatment to remove natural organic matters and biopolymer foulants. *Water Res.* **2021**, *195*, 117010.
- (17) Chuang, Y.-H.; Mitch, W. A. Effect of Ozonation and Biological Activated Carbon Treatment of Wastewater Effluents on Formation of N-nitrosamines and Halogenated Disinfection Byproducts. *Environ. Sci. Technol.* **2017**, *51*, 2329–2338.
- (18) Zheng, X.; Ernst, M.; Jekel, M. Pilot-scale investigation on the removal of organic foulants in secondary effluent by slow sand filtration prior to ultrafiltration. *Water Res.* **2010**, *44*, 3203–3213.
- (19) Lu, S.; Liu, J.; Li, S.; Biney, E. Analysis of up-flow aerated biological activated carbon filter technology in drinking water treatment. *Environ. Technol.* **2013**, *34*, 2345–2351.
- (20) Zhang, Z.; Xi, H.; Yu, Y.; Wu, C.; Yang, Y.; Guo, Z.; Zhou, Y. Coupling of membrane-based bubbleless micro-aeration for 2,4-dinitrophenol degradation in a hydrolysis acidification reactor. *Water Res.* **2022**, *212*, 118119.
- (21) Mei, X.; Guo, Z.; Liu, J.; Bi, S.; Li, P.; Wang, Y.; Shen, W.; Yang, Y.; Wang, Y.; Xiao, Y.; Yang, X.; Liu, Y.; Zhao, L.; Wang, Y.; Hu, S. Treatment of formaldehyde wastewater by a membrane-aerated biofilm reactor (MABR): The degradation of formaldehyde in the presence of the cosubstrate methanol. *Chem. Eng. J.* **2019**, *372*, 673–683.
- (22) Hou, D.; Jassby, D.; Nerenberg, R.; Ren, Z. J. Hydrophobic Gas Transfer Membranes for Wastewater Treatment and Resource Recovery. *Environ. Sci. Technol.* **2019**, *53*, 11618–11635.
- (23) Aybar, M.; Pizarro, G.; Boltz, J. P.; Downing, L.; Nerenberg, R. Energy-efficient wastewater treatment via the air-based, hybrid membrane biofilm reactor (hybrid MfBR). *Water Sci. Technol.* **2014**, *69*, 1735–1741.
- (24) Pucher, M.; Wünsch, U.; Weigelhofer, G.; Murphy, K.; Hein, T.; Graeber, D. staRdom: Versatile Software for Analyzing Spectroscopic Data of Dissolved Organic Matter in R. **2019**, *11* (11), 2366.
- (25) Park, M.; Snyder, S. A. Sample handling and data processing for fluorescent excitation-emission matrix (EEM) of dissolved organic matter (DOM). *Chemosphere* **2018**, *193*, 530–537.
- (26) Oksanen, J.; Simpson, G.; Blanchet, F.; Kindt, R.; Legendre, P.; Minchin, P.; O'Hara, R.; Solymos, P.; Stevens, M.; Szoecs, E.; Wagner, H. *Vegan: Community Ecology Package (R package version 2.6–2)*. 2022.
- (27) EPA., U. S. *Method 551.1: Determination of Chlorination Disinfection Byproducts, Chlorinated Solvents, and Halogenated Pesticides/Herbicides in Drinking Water by Liquid-Liquid Extraction and Gas Chromatography With Electron-Capture Detection*, Revision 1.0. USEPA: Cincinnati, OH. 1995.
- (28) EPA., U. S. *Method 552.3: Determination of haloacetic acids and dalapon in drinking water by liquid-liquid microextraction, derivatization, and Gas chromatography with electron capture detection*. EPA 815-B-03-002; USEPA. Revision 1.0. 2003.
- (29) Bradford, M. M. A rapid and sensitive method for the quantitation of microgram quantities of protein utilizing the principle of protein-dye binding. *Anal. Biochem.* **1976**, *72*, 248–254.
- (30) DuBois, M.; Gilles, K. A.; Hamilton, J. K.; Rebers, P. A.; Smith, F. Colorimetric Method for Determination of Sugars and Related Substances. *Anal. Chem.* **1956**, *28*, 350–356.
- (31) Chen, W.; Ren, K.; Isabwe, A.; Chen, H.; Liu, M.; Yang, J. Stochastic processes shape microeukaryotic community assembly in a subtropical river across wet and dry seasons. *Microbiome* **2019**, *7*, 138.

- (32) Afgan, E.; Baker, D.; Batut, B.; van den Beek, M.; Bouvier, D.; Čech, M.; Chilton, J.; Clements, D.; Coraor, N.; Grüning, B. A.; Guerler, A.; Hillman-Jackson, J.; Hiltemann, S.; Jalili, V.; Rasche, H.; Soranzo, N.; Goecks, J.; Taylor, J.; Nekrutenko, A.; Blankenberg, D. The Galaxy platform for accessible, reproducible and collaborative biomedical analyses: 2018 update. *Nucleic Acids Res.* **2018**, *46*, W537–W544.
- (33) Douglas, G. M.; Maffei, V. J.; Zaneveld, J. R.; Yurgel, S. N.; Brown, J. R.; Taylor, C. M.; Huttenhower, C.; Langille, M. G. I. PICRUSt2 for prediction of metagenome functions. *Nat. Biotechnol.* **2020**, *38*, 685–688.
- (34) Ren, Y.; Yu, G.; Shi, C.; Liu, L.; Guo, Q.; Han, C.; Zhang, D.; Zhang, L.; Liu, B.; Gao, H.; Zeng, J.; Zhou, Y.; Qiu, Y.; Wei, J.; Luo, Y.; Zhu, F.; Li, X.; Wu, Q.; Li, B.; Fu, W.; Tong, Y.; Meng, J.; Fang, Y.; Dong, J.; Feng, Y.; Xie, S.; Yang, Q.; Yang, H.; Wang, Y.; Zhang, J.; Gu, H.; Xuan, H.; Zou, G.; Luo, C.; Huang, L.; Yang, B.; Dong, Y.; Zhao, J.; Han, J.; Zhang, X.; Huang, H. Majorbio Cloud: A one-stop, comprehensive bioinformatic platform for multiomics analyses. *iMeta* **2022**, No. e12.
- (35) Krzywinski, M.; Schein, J.; Birol, I.; Connors, J.; Gascoyne, R.; Horsman, D.; Jones, S. J.; Marra, M. A. Circos: an information aesthetic for comparative genomics. *Genome Res.* **2009**, *19*, 1639–1645.
- (36) Team, R. C. R: *A language and environment for statistical computing*; R Foundation for Statistical Computing: Vienna, Austria. 2022.
- (37) Benner, J.; Helbling, D. E.; Kohler, H.-P. E.; Wittebol, J.; Kaiser, E.; Prasse, C.; Ternes, T. A.; Albers, C. N.; Aamand, J.; Horemans, B.; Springael, D.; Walravens, E.; Boon, N. Is biological treatment a viable alternative for micropollutant removal in drinking water treatment processes? *Water Res.* **2013**, *47*, 5955–5976.
- (38) Ritson, J. P.; Graham, N. J. D.; Templeton, M. R.; Clark, J. M.; Gough, R.; Freeman, C. The impact of climate change on the treatability of dissolved organic matter (DOM) in upland water supplies: A UK perspective. *Sci. Total Environ.* **2014**, *473-474*, 714–730.
- (39) Shakil, S.; Tank, S. E.; Kokelj, S. V.; Vonk, J. E.; Zolkos, S. Particulate dominance of organic carbon mobilization from thaw slumps on the Peel Plateau, NT: Quantification and implications for stream systems and permafrost carbon release. *Environ. Res. Lett.* **2020**, *15*, No. 114019.
- (40) Kida, M.; Kojima, T.; Tanabe, Y.; Hayashi, K.; Kudoh, S.; Maie, N.; Fujitake, N. Origin, distributions, and environmental significance of ubiquitous humic-like fluorophores in Antarctic lakes and streams. *Water Res.* **2019**, *163*, 114901.
- (41) McKnight, D. M.; Boyer, E. W.; Westerhoff, P. K.; Doran, P. T.; Kulbe, T.; Andersen, D. T. Spectrofluorometric characterization of dissolved organic matter for indication of precursor organic material and aromaticity. *Limnology and Oceanography* **2001**, *46*, 38–48.
- (42) Huguet, A.; Vacher, L.; Relexans, S.; Saubusse, S.; Froidefond, J. M.; Parlanti, E. Properties of fluorescent dissolved organic matter in the Gironde Estuary. *Org. Geochem.* **2009**, *40*, 706–719.
- (43) Liu, M.; Siddique, M. S.; Graham, N. J. D.; Yu, W. Removal of Small-Molecular-Weight Organic Matter by Coagulation, Adsorption, and Oxidation: Molecular Transformation and Disinfection By-product Formation Potential. *ACS ES&T Engineering* **2022**, *2*, 886–894.
- (44) Mesfioui, R.; Love, N. G.; Bronk, D. A.; Mulholland, M. R.; Hatcher, P. G. Reactivity and chemical characterization of effluent organic nitrogen from wastewater treatment plants determined by Fourier transform ion cyclotron resonance mass spectrometry. *Water Res.* **2012**, *46*, 622–634.
- (45) Smith, C. R.; Sleighter, R. L.; Hatcher, P. G.; Lee, J. W. Molecular Characterization of Inhibiting Biochar Water-Extractable Substances Using Electrospray Ionization Fourier Transform Ion Cyclotron Resonance Mass Spectrometry. *Environ. Sci. Technol.* **2013**, *47*, 13294–13302.
- (46) Ohno, T.; He, Z.; Sleighter, R. L.; Honeycutt, C. W.; Hatcher, P. G. Ultrahigh Resolution Mass Spectrometry and Indicator Species Analysis to Identify Marker Components of Soil- and Plant Biomass-Derived Organic Matter Fractions. *Environ. Sci. Technol.* **2010**, *44*, 8594–8600.
- (47) Yuan, Z.; He, C.; Shi, Q.; Xu, C.; Li, Z.; Wang, C.; Zhao, H.; Ni, J. Molecular Insights into the Transformation of Dissolved Organic Matter in Landfill Leachate Concentrate during Biodegradation and Coagulation Processes Using ESI FT-ICR MS. *Environ. Sci. Technol.* **2017**, *51*, 8110–8118.
- (48) Reshmy, R.; Athiyaman Balakumaran, P.; Divakar, K.; Philip, E.; Madhavan, A.; Pugazhendhi, A.; Sirohi, R.; Binod, P.; Kumar Awasthi, M.; Sindhu, R. Microbial valorization of lignin: Prospects and challenges. *Bioresour. Technol.* **2022**, *344*, 126240.
- (49) Gnowe, W. D.; Noubissié, E.; Noumi, G. B. Influence of time and oxygenation on the degradation of organic matter, nitrogen and phosphates during the biological treatment of slaughterhouse effluent. *Case Stud. Chem. Environ. Eng.* **2020**, *2*, 100048.
- (50) Boye, K.; Noël, V.; Tfaily, M. M.; Bone, S. E.; Williams, K. H.; Bargar, J. R.; Fendorf, S. Thermodynamically controlled preservation of organic carbon in floodplains. *Nat. Geosci.* **2017**, *10*, 415–419.
- (51) Kellerman, A. M.; Kothawala, D. N.; Dittmar, T.; Tranvik, L. J. Persistence of dissolved organic matter in lakes related to its molecular characteristics. *Nat. Geosci.* **2015**, *8*, 454–457.
- (52) Ma, J.; Gao, M.; Liu, Q.; Wang, Q. High efficiency three-dimensional electrochemical treatment of amoxicillin wastewater using Mn–Co/GAC particle electrodes and optimization of operating condition. *Environ. Res.* **2022**, *209*, 112728.
- (53) Coşkun, M. İ.; Karahan, İ. H.; Golden, T. D. Computer assisted corrosion analysis of hydroxyapatite coated CoCrMo biomedical alloys. *Surf. Coat. Technol.* **2015**, *275*, e1–e9.
- (54) Reguera, G.; McCarthy, K. D.; Mehta, T.; Nicoll, J. S.; Tuominen, M. T.; Lovley, D. R. Extracellular electron transfer via microbial nanowires. *Nature* **2005**, *435*, 1098–1101.
- (55) Gorby, Y. A.; Yanina, S.; McLean, J. S.; Rosso, K. M.; Moyles, D.; Dohnalkova, A.; Beveridge, T. J.; Chang, I. S.; Kim, B. H.; Kim, K. S.; Culley, D. E.; Reed, S. B.; Romine, M. F.; Saffarini, D. A.; Hill, E. A.; Shi, L.; Elias, D. A.; Kennedy, D. W.; Pinchuk, G.; Watanabe, K.; Ishii, S. I.; Logan, B.; Nealson, K. H.; Fredrickson, J. K. Electrically conductive bacterial nanowires produced by Shewanella oneidensis strain MR-1 and other microorganisms. *Proc. Natl. Acad. Sci. U. S. A.* **2006**, *103*, 11358–11363.
- (56) Boschker, H. T. S.; Cook, P. L. M.; Polerecky, L.; Eachambadi, R. T.; Lozano, H.; Hidalgo-Martinez, S.; Khalenkov, D.; Spaminato, V.; Claes, N.; Kundu, P.; Wang, D.; Bals, S.; Sand, K. K.; Cavezza, F.; Hauffmann, T.; Bjerg, J. T.; Skirtach, A. G.; Kochan, K.; McKee, M.; Wood, B.; Bedolla, D.; Gianoncelli, A.; Geerlings, N. M. J.; Van Gerven, N.; Remaut, H.; Geelhoed, J. S.; Millan-Solsona, R.; Fumagalli, L.; Nielsen, L. P.; Franquet, A.; Manca, J. V.; Gomila, G.; Meysman, F. J. R. Efficient long-range conduction in cable bacteria through nickel protein wires. *Nat. Commun.* **2021**, *12*, 3996.
- (57) Wang, H.; Zheng, Y.; Zhu, B.; Zhao, F. In situ role of extracellular polymeric substances in microbial electron transfer by *Methylomonas* sp. LW13. *Fundamental Res.* **2021**, *1*, 735–741.
- (58) Sloan, W. T.; Lunn, M.; Woodcock, S.; Head, I. M.; Nee, S.; Curtis, T. P. Quantifying the roles of immigration and chance in shaping prokaryote community structure. *2006*, *8* (4), 732–740, DOI: [10.1111/j.1462-2920.2005.00956.x](https://doi.org/10.1111/j.1462-2920.2005.00956.x).
- (59) Newton, R. J.; Jones, S. E.; Eiler, A.; McMahon, K. D.; Bertilsson, S. A guide to the natural history of freshwater lake bacteria. *Microbiology and Molecular Biology Reviews* **2011**, *75*, 14–49.
- (60) Lu, Z.; Sun, W.; Li, C.; Cao, W.; Jing, Z.; Li, S.; Ao, X.; Chen, C.; Liu, S. Effect of granular activated carbon pore-size distribution on biological activated carbon filter performance. *Water Res.* **2020**, *177*, 115768.
- (61) Šimek, K.; Horňák, K.; Ježbera, J.; Nedoma, J.; Vrba, J.; Stráskrábová, V.; Macek, M.; Dolan, J. R.; Hahn, M. W. Maximum growth rates and possible life strategies of different bacterioplankton groups in relation to phosphorus availability in a freshwater reservoir. *Environ. Microbiol.* **2006**, *8*, 1613–1624.

- (62) Lautenschlager, K.; Hwang, C.; Ling, F.; Liu, W.-T.; Boon, N.; Köster, O.; Egli, T.; Hammes, F. Abundance and composition of indigenous bacterial communities in a multi-step biofiltration-based drinking water treatment plant. *Water Res.* **2014**, *62*, 40–52.